

WGAN-LUNet for High-Accuracy Lung Nodule Segmentation

Narendra Lalchand Lokhande*, Tushar Hrishikesh Jaware

Department of Electronics and Telecommunication, R C Patel Institute of Technology, Shirpur, 425405, Maharashtra, India.
*Corresponding Author's Email: narenlokhande@gmail.com

Abstract

In the realm of computer-aided diagnosis systems designed for lung cancer, accurately segmenting nodules holds vital importance. This segmentation process has a vital role in examining the image attributes of lung nodules captured in computed tomography scans, ultimately aiding in separation of benign and cancerous nodules. Timely detection of these lesions stands as the most effective strategy in combating lung cancer, a disease notorious for its high malignancy rates across both genders. Despite numerous deep learning techniques proposed for nodule segmentation, it remains challenging due to factors such as nodule characteristics, location, false positives, and the necessity for precise boundary detection. The present paper presents an ultra-modern method for lung nodule segmentation in computer tomographic images, based on a Generative Adversarial Network. A discriminator and a generator make up the GAN model. Our generator, Residual Dilated Attention Gate UNet, serves as the segmentation module, while a discriminator is Convolutional Neural Network classifier. To enhance training stability, we utilize the Wasserstein GAN algorithm. We compare our hybrid deep learning model, called WGAN-LUNet, both quantitatively and qualitatively with other methods that are already in use. We evaluate the model using multiple quantitative criteria.

Keywords: Deep Learning, Generative Adversarial Network (GAN), Lung nodule, Residual dilated Attention Gate UNet, Segmentation.

Introduction

Lung cancer is second most serious disease which cause death and most frequently detected cancer in men (1). Detecting lung nodules early is crucial for lowering mortality rates among lung cancer patients since the chances of a successful cure drastically diminish once clinical symptoms of lung cancer manifest (2). Early diagnosis is one approach to significantly increase the survival rate. Computed tomography (CT) imaging and X-rays are the main non-invasive methods used to diagnose lung cancer. Other techniques include intrusive diagnostic procedures like biopsies, which may harm surrounding tissues. The most often utilised test modality for examining and diagnosing lung cancer is CT imaging. According to NLST Research Team (3) death rate was reduced by 20% when using CT imaging in contrast to non-CT imaging modalities. Nevertheless, due to advancements in scanner technology, computed tomography (CT) generates a substantial volume of images, posing a time-consuming and challenging task for radiologists to identify nodules within a

vast dataset. Figure 1 shows few lung CT images with their ground truth and their outline filled with colour. Due to the characteristics of lung nodule it may diagnose visual analysis imperfect subjectively and this task is also complex one. Hence, there is need of automated method of lung nodule localization and segmentation. Accurate segmentation of nodules on lung CT images is essential but challenging with traditional methods. A deep learning-based method using residual units and nested 3D convolutional networks was presented by Kido *et al.*, (4). They achieved accuracy (DS = 0.845, IoU = 0.738) compared to existing deep learning models. A double-path network utilizing residual blocks to extract local features and rich contextual information from nodules to enhance performance was proposed by Liu *et al.*, (5). However, their approach used a volume of interest fixed, limiting exploration of nodules and consequently leading to suboptimal performance. Ronneberger *et al.*, (6) developed method of segmentation known as U-Net

This is an Open Access article distributed under the terms of the Creative Commons Attribution CC BY license (<http://creativecommons.org/licenses/by/4.0/>), which permits unrestricted reuse, distribution, and reproduction in any medium, provided the original work is properly cited.

(Received 28th June 2024; Accepted 22nd October 2024; Published 30th October 2024)

especially for medical image, and U-Net gained widespread use. Since then, various improvements have been made to U-Net. For example, Tong *et al.*, (7) boosted U-Net's effectiveness in nodule extraction by using skip connections between its encoder-decoder paths. For segmentation of objects, a model Badrinarayan *et al.*, (8) proposed is SegNet. Similar to UNET, SegNet also has encoding and decoding structure except instead of convolution transpose it uses unpooling and does not have skip connections. Advanced GAN-based algorithm WGAN-RDA-UNET proposed by Negi *et al.*, (9), for tumor segmentation in breast ultrasound images. Based on this study we have modified and tuned network for segmentation of nodules.

Building upon the framework proposed by Zhuang *et al.*, (10), which introduces a Residual Dilated-Attention-Gate-UNet, we incorporate it with

Wasserstein Generative Adversarial Networks (WGAN) to create a robust and precise nodule segmentation technique. Arjovsky *et al.*, (11) proposed WGAN with new loss metric with improved stabilization to converge the generator. The resulting deep learning model is termed WGAN-LUNet. Through our experimentation, we demonstrate that adversarial training enhances segmentation quality, producing outputs comparable to those of experts.

Methodology

Generative Adversarial Networks (GANs) are a breakthrough in machine learning, proposed by Goodfellow *et al.*, (12). The generator and discriminator neural networks participate in a game in which generator creates realistic data and discriminator distinguishes between real and fake data.

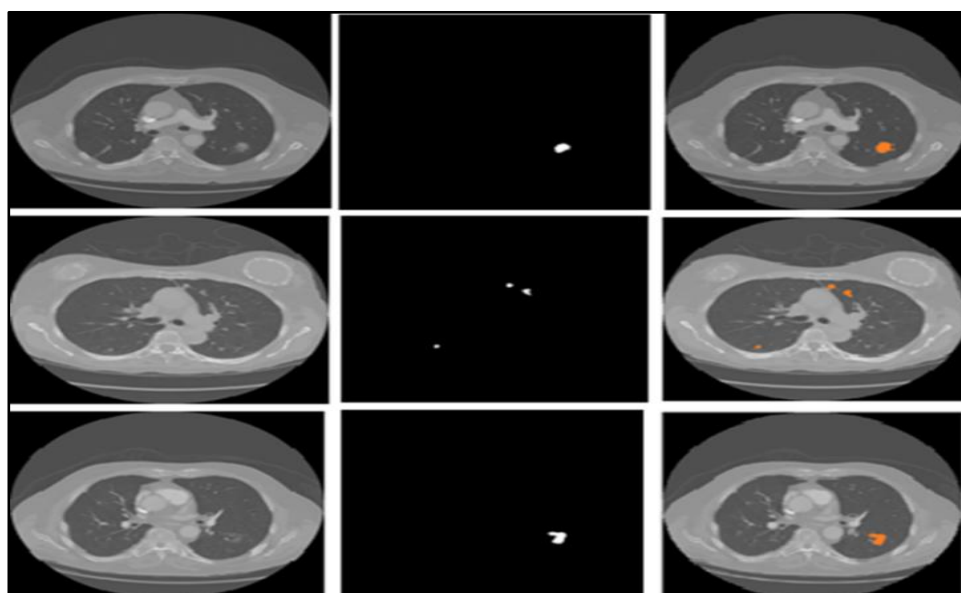


Figure 1: Left-Lung CT Images with Nodule, Middle- Ground Truth and Right- Marked Nodules with Ground Truth

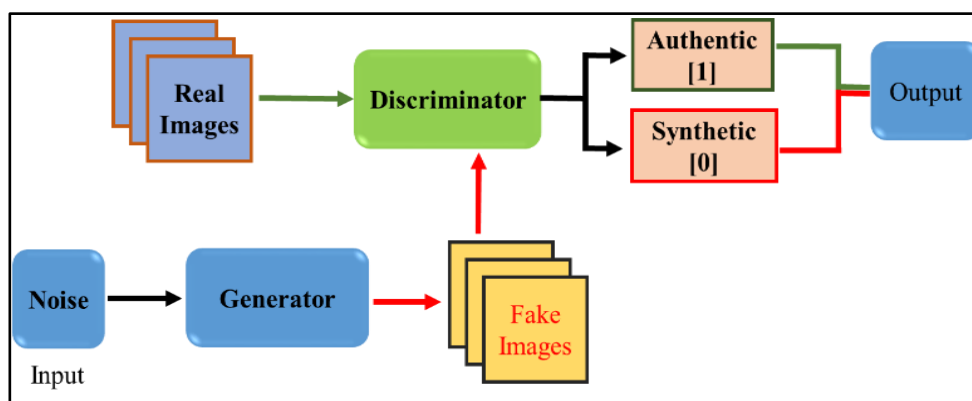


Figure 2: Traditional Generative Adversarial Network

Figure 2 illustrate traditional Generative Adversarial Network. Iterative process of network training as a min-max kind of competitive learning among discriminator-D and generator-G is shown

$$\frac{\min}{G} \frac{\max}{D} V(G, D) = E_{x \sim P_{data}(x)} [\log \log D(x)] + E_{z \sim P_z(z)} [\log \log (1 - D(G(z)))] \quad [1]$$

by Eq. [1]. In the equation, $D(x)$ – output showing probability of x being real P_z - generated data distribution P_{data} - real data and z - Random number.

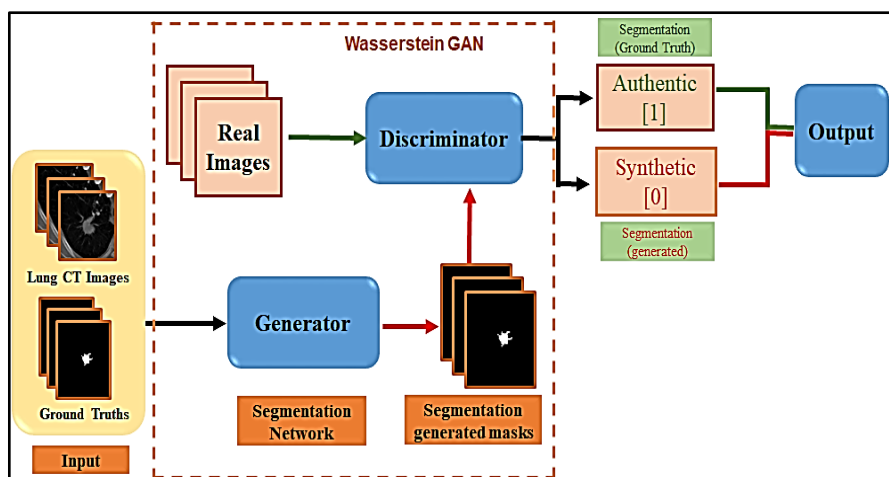


Figure 3: Proposed WGAN-LUNet Architecture

The devised WGAN-LUNet framework leverages the aforementioned concept to delineate lung nodule in CT images. In this architecture, the segmentation model, trained on data, functions as the generator, generating segmented regions. Simultaneously, an adversarial network discerns among generated segmentation outputs and ground truth annotations. This training scheme of adversarial facilitates refinement of the segmentation model's performance, enhancing its ability to accurately delineate lung nodules in CT scans. In this approach, we utilize the RDA-UNET proposed by Zhuang *et al.*, (10) as the segmentation generator, while fully connected CNN network as the discriminator. This combined framework forms the WGAN-LUNet architecture. Illustrated in Figure 3, this architecture effectively identifies and corrects discrepancies at higher semantic levels between the segmented lesion outputs generated by the generator and the ground truth annotations. Through this corrective mechanism, WGAN-LUNet enhances the accuracy of segmentation results, closely matching the annotations provided by domain experts, thereby ensuring high fidelity.

Generator

As a segmentation model, the generator combines Attention Gate (AG) techniques Dilation

Convolution modules, and Residual Networks in a U-Net architecture. Input to this model includes CT images of lung nodules along with their corresponding ground truth annotations, while the output comprises predicted segmentation masks generated by RDA-U-Net. Primary aim of the generator is to produce synthetic images, specifically lesion maps of input CT images, which can deceive the discriminator into perceiving them as genuine. Illustrated in Figure 4 shows architecture of generator network, resembling the model described in by Negi *et al.*, (9). It encompasses seven residual nets for extracting crucial features from CT images, with Reduced-size feature maps forwarded to a dilated convolution module. The inclusion of dilation convolutions and residual units mitigates issues such as fading gradients while training and enhances receptive field, correspondingly. Following forward pass, the output is fed into an up-sampling process comprising six residual networks, each featuring an individual AG to focus study on nodule region apart from non-nodule areas. Ultimately, generator outputs a segmentation mask in binary via convolution layer in last, indicating classification label for every pixel. Eq. [10] is used for generators training.

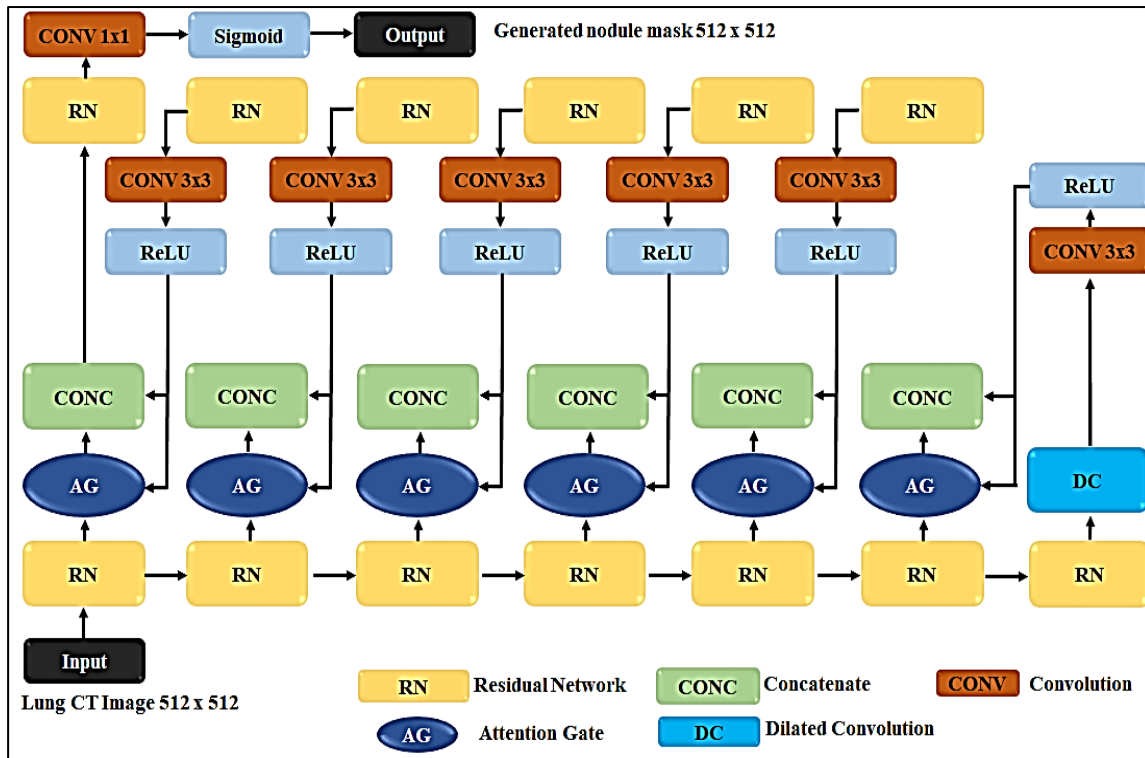


Figure 4: Architecture of the Generator

Discriminator

One of the most pivotal component within the GAN framework is discriminator, tasked with discerning the authenticity of the presented instances. In the proposed architecture, the discriminator model adopts a classification network design. It comprises a CNN structure with twelve convolution layers and unique fully connected layer for final classification. Each layer of convolutional is accompanied by a leaky ReLU activation and layer of max-pooling for down sampling, fostering feature extraction. Furthermore, batch normalization is integrated to regularize and expedite training process, given the critical impact of the discriminator's performance on efficacy of adversarial loss.

During training, discriminator receives segmented nodule results (fake/false) generated by generator

and annotations (real, true) as input samples, provided in one-hot encoding format. As a result, the binary output of the discriminator specifies whether the input corresponds to the generated segmentation result from the generator or to a ground truth from the training set. At an image level, the model categorises the authenticity of the input, assigning a value of 1 for real and 0 for fake. Illustrated in Figure 5, we employ an Adam optimizer with a learning rate set to 0.0001 for training the discriminator. The chosen loss function is BCE (Binary Cross Entropy), which effectively manages discrepancies between segmentation result and ground truth. To ensure improvement in overall accuracy of segmentation process this loss function is computed using generated segmentation output and ground truths. In the Eq. [2] p - predicted probability value and y - real value.

$$Loss = -(y \cdot \log \log (p) + (1 - y) \cdot \log \log (1 - p)) \quad [2]$$

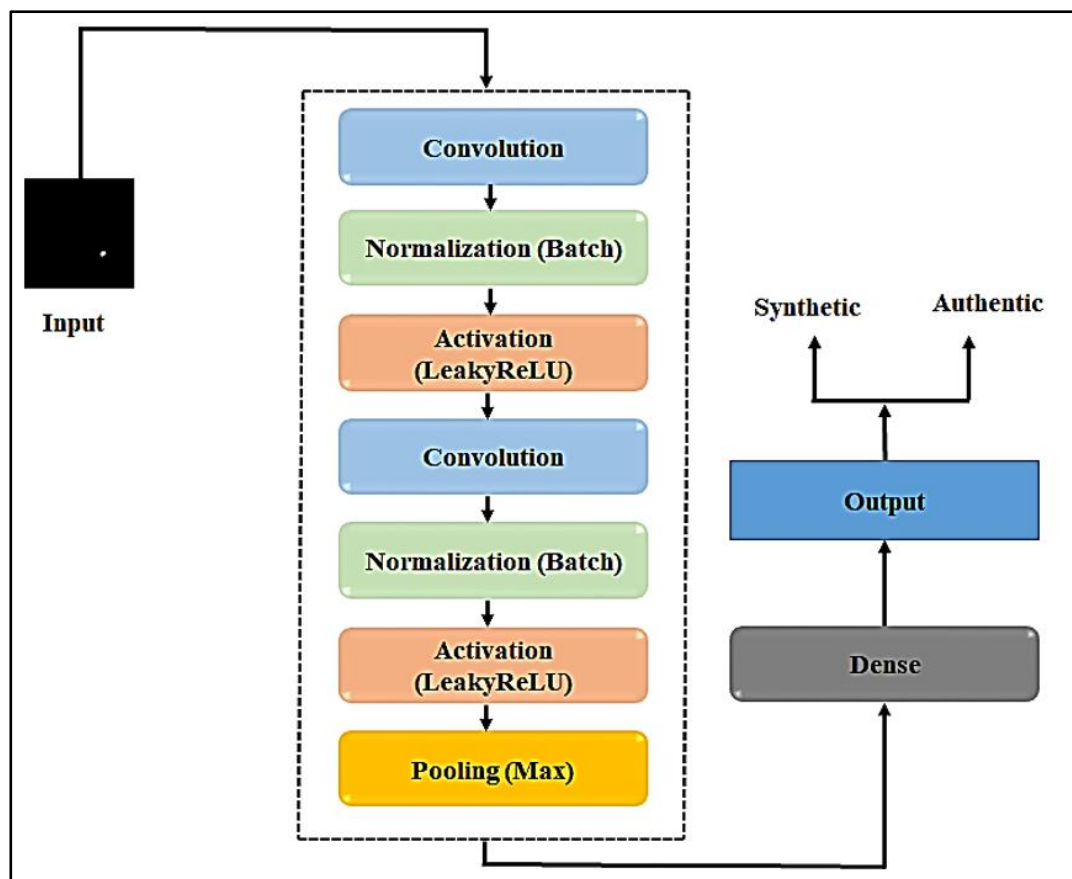


Figure 5: Architecture of the Discriminator

LUNet-WGAN

The unified model is created when the generator and discriminator are combined, denoted as LUNet-WGAN. Within this integrated framework, CT images of lung nodules serve as input, while their corresponding ground truth annotations act as labels. Initially, a batch of CT images is fed into the generator to produce segmentation maps. The discriminator then receives segmentation maps with the corresponding ground truth labels, providing final output for combined model. Figure 3 shows schematic depiction of this data flow. This concise framework outlines the essential steps for implementing a GAN-based model in lung nodule segmentation, focusing on data preparation, architecture, training, evaluation, and model refinement.

Dataset Preparation: Collect a dataset of lung CT scans with annotated nodule segmentations.

Model Architecture: Choose a GAN architecture with a U-Net-based generator for detailed feature

capture and a PatchGAN discriminator for local and global evaluation of segmentation quality.

Training: Train the GAN using paired data. Employ a combination of adversarial loss and traditional losses like Dice loss or Binary Cross-Entropy to ensure accurate segmentation.

Evaluation: Assess the model using metrics such as accuracy, Sensitivity, Specificity, Dice Score, DSC loss, IoU, F1-Score, PR-AUC and ROC-AUC to evaluate segmentation accuracy and performance.

Refinement: Fine-tune the GAN by adjusting loss weights, learning rates, or integrating additional feature extraction networks to enhance segmentation quality and reliability.

The objective function becomes crucial in adversarial training. The Wasserstein Generative Adversarial Network (WGAN), which selects a different objective function than traditional GANs, is used in this situation. Compared to traditional GANs, WGAN produces a more stable learning process by calculating the Wasserstein distance among segmentation result and ground truth.

Unlike the minimum maximum type competitive learning described in Eq. [1], WGAN competitive

learning between generator-G and discriminator-D can be stated as:

$$\frac{\min}{G} \frac{\max}{D} V(G, D) = E_{x \sim P_{data}(x)} [\log \log D(x)] + E_{z \sim P_Z(z)} [\log \log (1 - D(G(z)))] \quad [3]$$

Where $D(x)$ is discriminator output that indicates the likelihood that x is real, P_{data} is the real data distribution, p_z is the distribution of generated data, and z is a random number. In this instance, x will be the segmented output of the generator, and input CT image is z . The discriminator is penalised for inaccurate classification by loss function, which also penalises deviation between segmented results and ground truth. This guarantees that two networks remain stable and do not become dominant over one another. WGAN leverages the Wasserstein distance, which provides smoother gradients and more stable training compared to traditional GANs using Jensen-Shannon divergence. This stability prevents mode collapse, ensuring the generator learns diverse nodule shapes and sizes, which is crucial for accurate lung nodule segmentation. The Wasserstein distance also better handles limited and imbalanced datasets, common in medical imaging, enabling WGAN to produce clinically meaningful segmentations with fewer artifacts and improved boundary precision. This makes WGAN a superior choice for capturing subtle and complex nodule variations.

Training Scheme

Main aim of suggested model is to obtain ultra-modern segmentation outcomes. Initial network instability may cause problems with parameter modification if generator and discriminator are both trained from scratch. To address this issue, generator model undergoes partial training separately. In the unified model, LUNet-WGAN undergoes adversarial training. First,

discriminator is built and previously trained generator is loaded. Subsequently, collective model undergoes training. This training process iterates with interchanging rounds of generator and discriminator. Initially, discriminator is trained for single step, followed by parameter updates and gradient propagation to compute adversarial loss. Then, discriminator is frozen, and combined net undergoes one-step training. Both models are then evaluated against validation set. This iterative cycle continues, reflecting the min-max concept outlined in Eq. [3]. With each and every cycle generator network become more accurate and reliable due to adversarial loss's training effect. Generator and discriminator parameter updates hinge on the discriminator's classification performance. The discriminator's parameters are modified if it is unable to distinguish between created and real data; if it is successful, the generator's parameters are adjusted. To achieve precise segmentation and fool the discriminator, the generator optimizes its parameters by leveraging both the discriminator's performance and its own loss. Segmentation results for the test data set are shown in Figure 6.

Evaluation Parameter

The effectiveness of the suggested method is quantitatively assessed using metrics like accuracy. It is a fundamental attribute denoting correctness and is frequently utilized as the primary evaluation criterion. Apart from accuracy other evaluation parameters such as Sensitivity, Specificity, Precision, F1score, ROC, Dice similarity coefficient, PR-AUC.

$$\text{Accuracy} = \frac{TP + TN}{TP + TN + FP + FN} \quad [4]$$

$$\text{Sensitivity} = \frac{TP}{TP + FN} \quad [5]$$

$$\text{Specificity} = \frac{TN}{TN + FP} \quad [6]$$

$$\text{Precision} = \frac{TP}{TP + FP} \quad [7]$$

$$\text{F1score} = 2 \times \frac{(\text{Precision} * \text{Sensitivity})}{(\text{Precision} + \text{Sensitivity})} \quad [8]$$

$$\text{DSCloss} = 1 - \text{DSC} \quad [9]$$

$$DSC = \frac{2 \times TP}{TP + TN + FP + FN} \quad [10]$$

$$IOU = \frac{|G \cap P|}{|G \cup P|} \quad [11]$$

Sensitivity is defined as percentages of real positives that are recognised as positive. Whereas Specificity is measure of real negatives that are recognised as negative. When FP is high, precision serves as an effective measurement index. Which is proportion of true positive to all positive values. When there is an uneven distribution of classes, the F1score is utilised. ROC can adjust the sensitivity of detection. The PR curve is the area under precision recall and AUC. Low false positive and false negative rates are indicated by high PR-AUC value. Ideally it is 1 which means error probability is 0. The capability of separating affected area from non-affected area is measured

by ROC-AUC. Higher value of ROC-AUC denotes better segmentation. Ideally which is 1.

The intersection over union, or IoU, is defined as the area of overlap between the predicted segmentation and the ground truth divided by the area of union between them. Range of IoU varies from 0 to 1. Value zero- no overlap while one - perfectly overlapping segmentation. Dice similarity coefficient is used to assess segmentation tasks, this metric is most commonly utilised. It indicates similarity or match between ground truth and segment predicted. Dice loss is defined by Eq. [9]. It expected to have value of DSC is 1 and DSCloss to be 0.

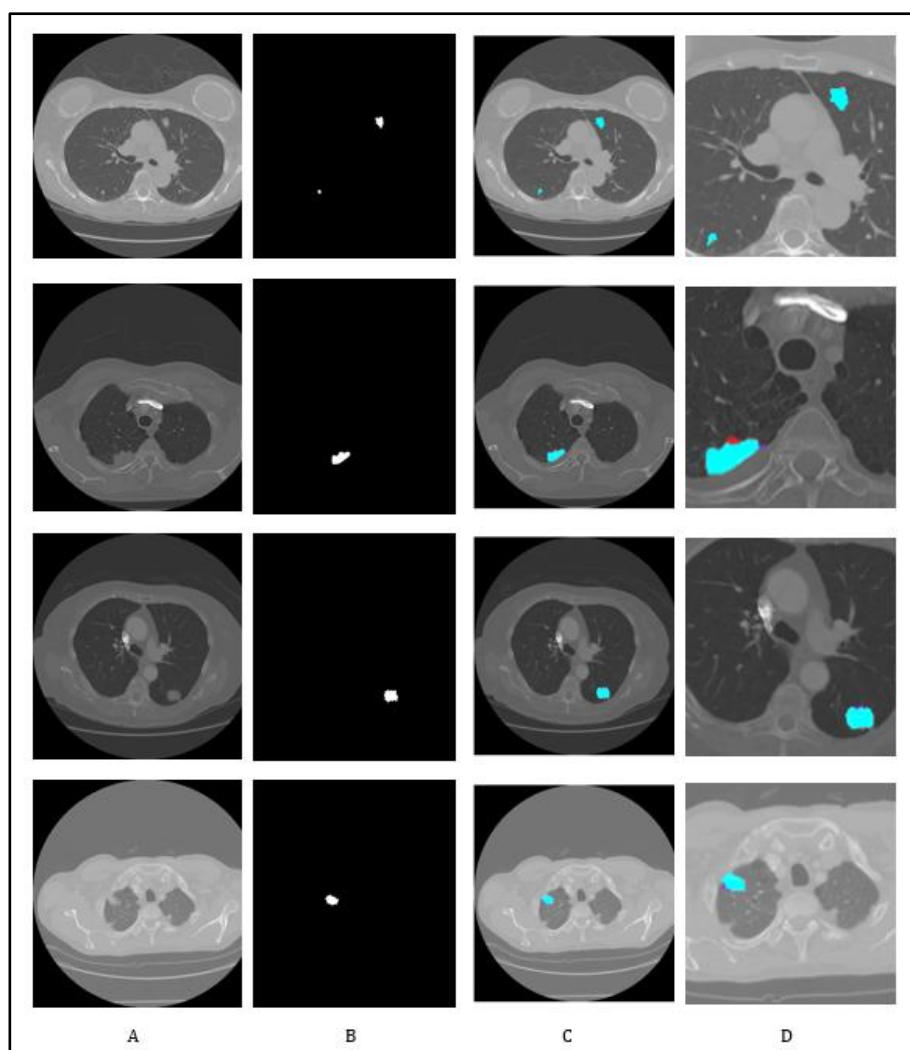


Figure 6: Segmentation Results Column A, B, C, D Shows Original Lung CT Images, Ground Truth, Segmented Lung Nodule Region and Scaled Up View of Nodule. Areas Indicated in Cyan Denote Where Predicted Segmentation and Ground Truth Intersect, Red Indicates Lesion Area that was Not Anticipated to be a Lesion, and Purple Indicates Non-Lesion Regions that the Model Categorized as Lesions.

WGAN offers several research benefits for lung nodule segmentation:

Improved Training Stability: Utilizes the Wasserstein distance for stable, non-saturating gradients, avoiding issues like vanishing gradients and unstable training seen in conventional GANs.

Reduced Mode Collapse: Encourages the generation of diverse outputs, capturing complex nodule shapes and variations with higher fidelity, which is critical for accurate segmentation.

Better Performance on Limited Data: Handles small and imbalanced datasets effectively, minimizing overfitting and achieving robust performance even with constrained data availability.

Enhanced Boundary Precision: Produces sharper and more accurate segmentation boundaries, reducing artifacts and improving delineation of nodule margins in medical images.

Integration of Domain Knowledge: Easily incorporates medical constraints (e.g., shape priors) to ensure clinically relevant segmentation results that are interpretable and aligned with clinical expectations.

Results and Discussion

The LIDC dataset (13) is most extensive publicly available collection of CT images designed for evaluating lung nodule segmentation and classification capabilities. It comprises 1,018 cases sourced from seven academic institutions and eight medical imaging companies worldwide.

Table 1: Model Parameter

Model	Total parameters	Trainable parameters
LUNet-WGAN	28816811	24079536
Generator	24098410	24079536
Discriminator	4718401	4714433

The proposed model was quantitatively evaluated against FCN8s, SegNet, U-Net, and RDAU-net using the metrics using Eq. [4] to Eq. [11]. Table 1 shows

Table 2: Evaluation Parameter

Metric	FCN8s (14)	UNET (6)	Segnet (8)	RDA-UNET (9)	Proposed Method
Accuracy	0.9551	0.9779	0.9756	0.9791	0.9807
Sensitivity	0.7088	0.8445	0.8369	0.8363	0.8838
Specificity	0.9688	0.9907	0.9801	0.9926	0.9936
Precision	0.6127	0.8262	0.8140	0.8863	0.9120
Loss	0.3527	0.1768	0.1827	0.1530	0.1165
DSC	0.6472	0.8031	0.8120	0.8461	0.8833
IOU	0.7013	0.7983	0.8015	0.8053	0.8713

- Total CT Scans: Approximately 1,000 CT scans.
- Total Nodules: Over 1,200 annotated nodules across the dataset.
- Distribution of Nodule Sizes:
 - < 10 mm: ~60%
 - 10-20 mm: ~25%
 - 20-30 mm: ~10%
 - 30 mm: ~5%
- Nodule Type Distribution:
 - Solid: ~60%
 - Part-Solid: ~25%
 - Ground-Glass: ~15%

Each case includes clinical thoracic CT images and an XML file documenting segmentation results from a two-step image annotation process conducted by four experienced chest radiologists. Slice intervals range from 0.45 mm to 5.0 mm, with pulmonary nodule diameters spanning 2.03 mm to 38.12 mm. Each lung nodule can be segmented by up to four radiologists, with annotations focusing on nodules 3 mm or larger.

In this study, nodules larger than 3 mm (totalling approximately 893 pulmonary nodules) are selected for experimentation, excluding those smaller than 3 mm. To address the variability in segmentation results among the four radiologists, a 50% consensus criterion is applied to establish ground truth outlines. From the 893 nodules, 100 are chosen for performance evaluation.

model trainable and non-trainable parameters by network.

F1Score	0.6572	0.8352	0.8255	0.8605	0.8975
PR-AUC	0.9148	0.9261	0.9538	0.9227	0.9537
ROC-AUC	0.8061	0.8892	0.8803	0.8551	0.8920

Table 2 shows that our model outperforms the others in nearly all metrics on a test data that is 20% the size of training data. The proposed method demonstrates superior performance across multiple evaluation metrics compared to traditional models such as FCN8s, UNET, Segnet, and RDA-UNET. It achieves the highest accuracy 0.9807, indicating its strong capability in correctly classifying both positive and negative cases. The sensitivity of the proposed model 0.8838 is also the highest among all methods, showcasing its effectiveness in detecting true positive cases and identifying lung nodules. In terms of specificity, the proposed method excels with a value of 0.9936, demonstrating its proficiency in accurately recognizing true negatives and minimizing false positives. The precision of 0.9120 further reflects the model's ability to distinguish true positives from negative cases, ensuring a lower rate of false positives.

Additionally, the proposed method has the lowest loss value 0.1165, highlighting its better optimization and convergence during training. It

achieves the highest Dice Similarity Coefficient (DSC) of 0.8833, which signifies a superior overlap between the predicted and actual segmentation regions, as well as the highest Intersection over Union (IoU) score of 0.8713, demonstrating precise segmentation results with minimal errors. The proposed method also shows the highest F1 score 0.8975, indicating a balanced performance in terms of precision and recall. Furthermore, the model achieves a PR-AUC of 0.9537, reflecting a high precision-recall balance and is comparable to other top-performing models. Although the ROC-AUC of the proposed method 0.8920 is slightly lower than UNET 0.8892, it still shows a good trade-off between sensitivity and specificity. Overall, the proposed WGAN-LUNet model consistently outperforms other models across all key metrics, including accuracy, sensitivity, specificity, precision, and DSC. These results suggest that WGAN-LUNet offers enhanced segmentation capabilities, making it a promising tool for clinical applications in lung nodule analysis and diagnostic support.

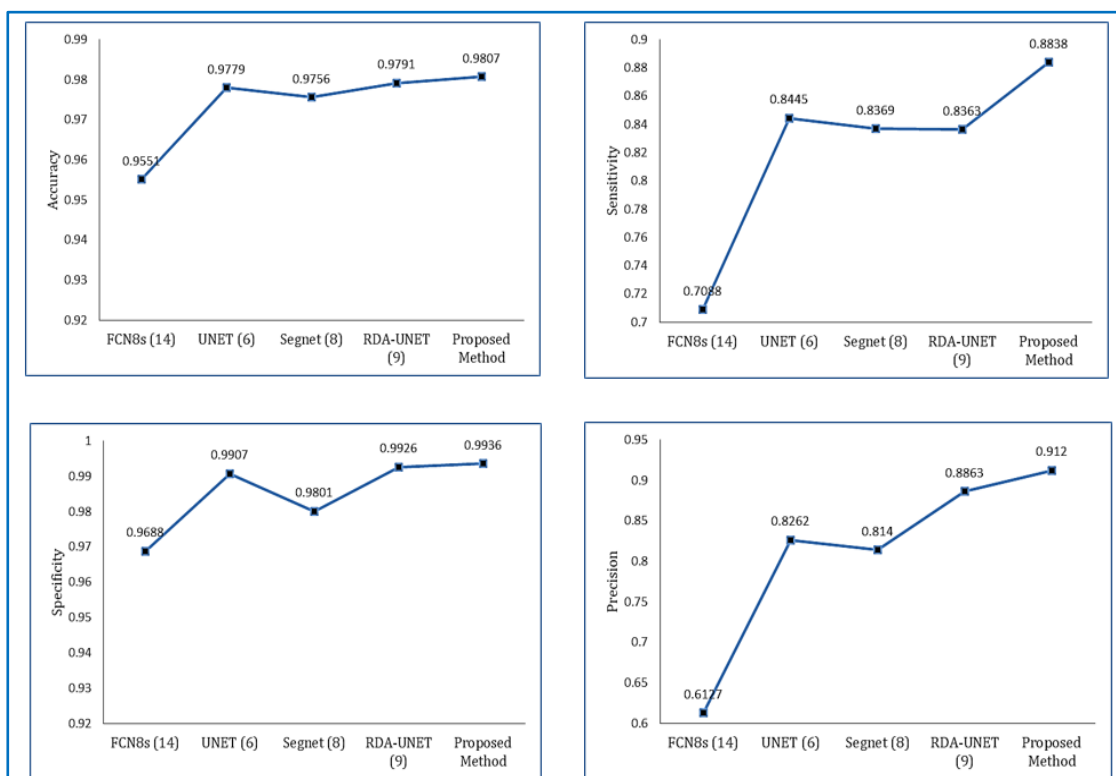


Figure 7: Comparison of Proposed Method Using Accuracy (Top Left), Sensitivity (Top Right), Specificity (Bottom Left) and Precision (Bottom Right)

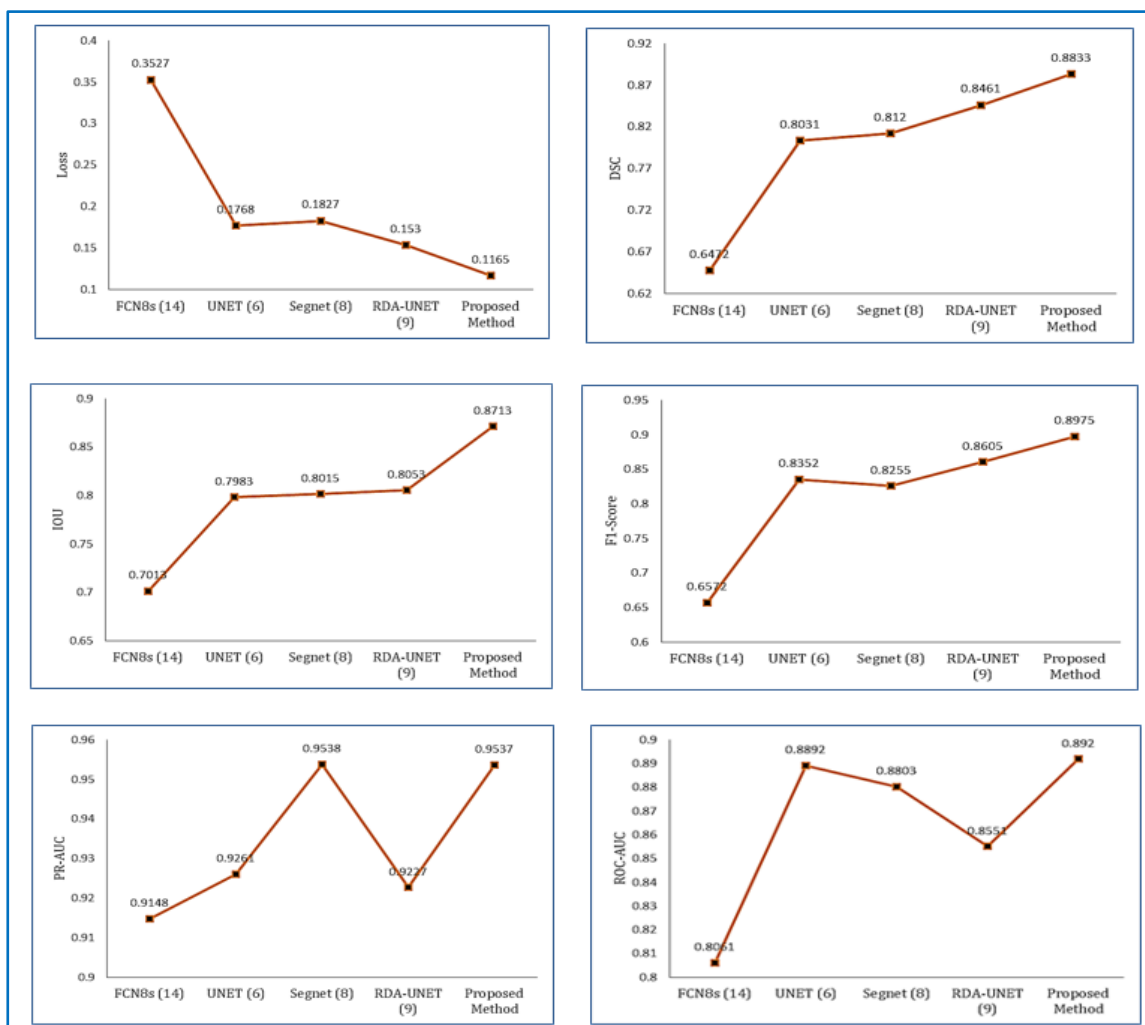


Figure 8: Comparison of Proposed Method Using Loss (Top Left), DSC (Top Right), IOU (Middle Left), F-1 Score (Middle Right), PR-AUC (Bottom Left) and ROC- AUC (Bottom Right)

Figure 7 illustrates comparison of proposed method using metrics accuracy, sensitivity, specificity and precision while Figure 8 shows comparison of proposed method using loss, DSC, IOU, F-1 Score, Pr-AUC, and RoC-AUC with four segmentation methods respectively. It is clear that

in segmentation tasks, U-Net designs perform better than FCNs and SegNet performs better than UNet. The ROC and PR curves for the WGAN on the testing dataset are displayed in Figure 9 and Figure 10. From comparison it is very clear that WGAN increases segmentation outcomes.

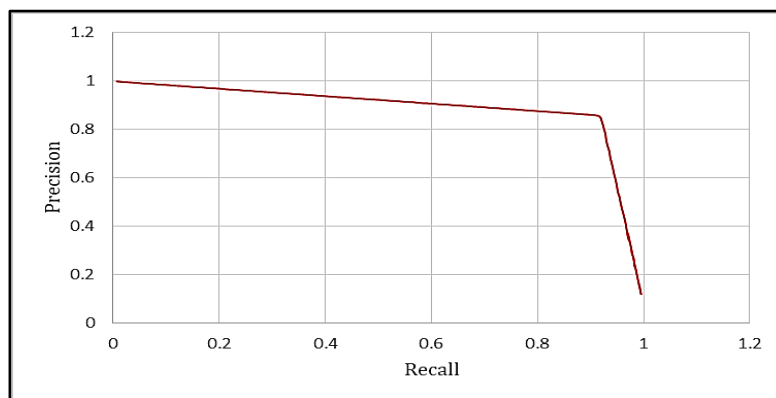


Figure 9: Precision-Recall Curve with AUC = 0.9537 of LUNet-WGAN

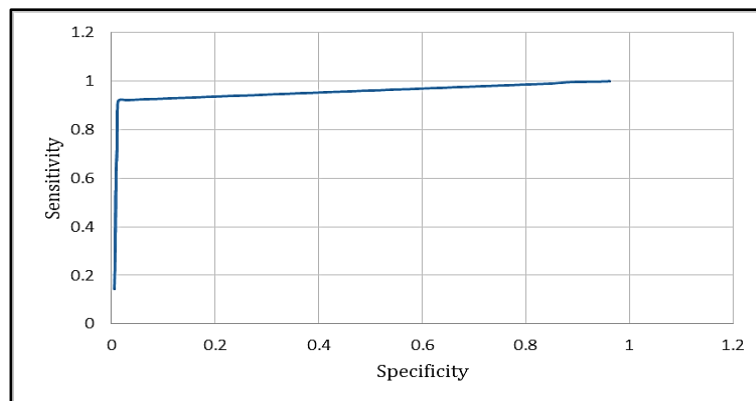


Figure 10: ROC Curve with AUC = 0.8920 of LUNet-WGAN

Generative Adversarial Networks (GANs) are increasingly used in image segmentation, improving performance despite challenges like non-convergence and gradient vanishing. This study introduces a novel WGAN-based approach for nodule segmentation in lung CT images, utilizing adversarial training to produce accurate nodule masks. Our method surpasses current techniques, enhancing precision by 3-4%, MeanIOU by 7-8%, and dice score by 4-5%. Hyperparameter tuning is crucial for optimal performance. Future research will extend this model to various medical imaging datasets to boost robustness.

Computational Complexity and Training Limitations of WGAN-LUNet: WGAN-LUNet, while offering improved segmentation performance, comes with increased computational complexity and longer training times compared to traditional models like U-Net. Following limitations occurred during training of WGAN-LUNet Model.

- Requires additional computations for Wasserstein distance calculation.
- Necessitates multiple discriminator updates for each generator update.
- Prolonged training durations due to the iterative nature of the adversarial updates.
- Higher memory consumption to accommodate the increased number of parameters and operations.
- Superior stability and reduced mode collapse compared to conventional models.
- Enhanced segmentation accuracy, particularly for complex nodule structures and variations that are challenging for traditional methods like U-Net.

Conclusion

The WGAN-LUNet model represents a substantial leap forward in lung nodule segmentation, overcoming the limitations associated with conventional methods. By utilizing the stability and robustness of Wasserstein GANs, WGAN-LUNet significantly improves segmentation accuracy and precision, especially when handling complex lung nodules in scenarios with limited and imbalanced datasets. The integration of this model into clinical workflows could streamline diagnostic processes, offering radiologists an advanced tool for accurate identification and analysis of lung nodules. Although the model entails higher computational complexity and longer training times, its ability to deliver superior segmentation quality and minimize artifacts makes it a valuable addition to medical imaging applications. Future efforts should focus on optimizing computational efficiency, enhancing the model's interpretability, and conducting extensive clinical validations to ensure its reliability and practical use in healthcare settings. Moreover, the development of web-based and mobile applications integrated into current clinical workflows could further enhance radiologists' efficiency, ultimately leading to improved patient outcomes and more effective treatment planning. To integrate WGAN-LUNet into clinical practice, the model must be optimized for seamless integration with existing radiology workflows and imaging software. This includes ensuring compatibility with various CT formats and maintaining interpretability of the results. By automating nodule segmentation and highlighting suspicious regions, WGAN-LUNet can support radiologists in providing second opinions and reducing diagnostic time, thereby enhancing

decision-making accuracy without disrupting routine clinical procedures.

Abbreviation

Nil.

Acknowledgment

Nil.

Author Contributions

Narendra Lalchand Lokhande: Conceptualization, experimentation, formal analysis, rough draft of manuscript, Tushar Hrishikesh Jaware: Supervision, writing reviews and editing.

Conflict of Interest

The authors declared that there are no conflicts of interest regarding the publication of this manuscript.

Ethics Approval

Not applicable.

Funding

No Funding received for research work.

References

1. Siegel RL, Miller KD, Wagle NS, Jemal A. Cancer Statistics, 2023. *CA Cancer J Clin.* 2023; 73(1):17–48.
2. Wu G, Woodruff HC, Shen J, Refaee T, Sanduleanu S, Ibrahim A, *et al.* Diagnosis of Invasive Lung Adenocarcinoma Based on Chest CT Radiomic Features of Part-Solid Pulmonary Nodules: A Multicenter Study. *Radiology.* 2020; 297(2):451–8.
3. The National Lung Screening Trial Research Team. Reduced Lung-Cancer Mortality With Low-Dose Computed Tomographic Screening. *N Engl J Med.* 2011; 365:395–409. <https://www.nejm.org/doi/full/10.1056/NEJMoa1102873>
4. Kido S, Kidera S, Hirano Y, Mabu S, Kamiya T, Tanaka N, *et al.* Segmentation Of Lung Nodules On CT Images Using A Nested Three-Dimensional Fully Connected Convolutional Network. *Front Artif Intell.* 2022; 5:782225.
5. Liu H, Cao H, Song E, Ma G, Xu X, Jin R, *et al.* A Cascaded Dual Pathway Residual Network For Lung Nodule Segmentation in CT Images. *Phys Med.* 2019; 63:112–21.
6. Ronneberger O, Fischer P, Brox T. U-Net: Convolutional Networks for Biomedical Image Segmentation. *Lecture Notes Comput Sci.* 2015; 9351:234–41.
7. Tong G, Li Y, Chen H, Zhang Q, Jiang H. Improved UNET Network for Pulmonary Nodules Segmentation. *Optik.* 2018;174:460–9.
8. Badrinarayanan V, Kendall A, Cipolla R. Segnet: A deep convolutional encoder-decoder architecture for image segmentation. *IEEE transactions on pattern analysis and machine intelligence.* 2017;39(12):2481-95.
9. Negi A, Raj ANJ, Nersisson R, Zhuang Z, Murugappan M. RDA-UNetWGAN: An Accurate Breast Ultrasound Lesion Segmentation Using Wasserstein Generative Adversarial Networks. *Arab J Sci Eng.* 2020; 45:6399–410.
10. Zhuang Z, Li N, Raj ANJ, Mahesh VGV, Qiu S. An RDAU-NET Model for Lesion Segmentation in Breast Ultrasound Images. *PLoS One.* 2019; 14(8):e0221535.
11. Arjovsky M, Chintala S, Bottou L. Wasserstein generative adversarial networks. In *International conference on machine learning.* PMLR. 2017;70:214-223.
12. Goodfellow I, Pouget-Abadie J, Mirza M, Xu B, Warde-Farley D, Ozair S, Courville A, Bengio Y. Generative adversarial nets. *Advances in neural information processing systems.* 2014;27:1-9.
13. Armato SG, McLennan G, Bidaut L, McNitt-Gray MF, Meyer CR, Reeves AP, *et al.* The Lung Image Database Consortium (LIDC) and Image Database Resource Initiative (IDRI): A Completed Reference Database of Lung Nodules on CT Scans. *Med Phys.* 2011; 38:915–31.
14. Long J, Shelhamer E, Darrell T. Fully convolutional networks for semantic segmentation. In *Proceedings of the IEEE conference on computer vision and pattern recognition.* 2015:3431-3440.